The Storm-Time Assessment of GNSS-SBAS Performance within African Equatorial and Low Latitude Region

O. E. Abe[1, 2], C. Paparini[1], R. H. Ngaya[1], X. Otero Villamide[1], S. M. Radicella[1], and B. Nava[1]

[1]TREGA Project Laboratory, Abdus Salam International Centre for theoretical Physics, Trieste, Italy
[2]Department of Physics, Federal University Oye-Ekiti, Ekiti State, Nigeria
Email: abeemman@yahoo.com

Abstract
A Satellite Based Augmentation System (SBAS) is designed to improve Global Navigation Satellite System (GNSS) in terms of integrity, accuracy, availability and continuity. Its performance depends among other factors on the conditions of the ionosphere. SBAS system performance is usually degraded after sunset hours during magnetically quiet-time periods in low-latitude regions. During geomagnetically disturbed periods the role of storm-time winds is important because they modify the atmospheric composition toward low latitudes. An index of ionospheric disturbance (DvTEC), the relative percentage of deviation of the vertical Total Electron Content (TEC) from the quiet level at each station was evaluated to study positive and negative phases of the storms. The rate of change of TEC index (ROTI) over all the stations was estimated to evaluate equatorial ionospheric gradients and irregularities. From the study it is observed that the positive deviations are more frequent than negative ones. The cases of moderate and minor storms studied in this paper showed that SBAS system performance during the disturbed periods depends on the local time in which the storm occurs, geographic longitude and other phenomena that need further study. During the storm-time conditions considered, three out of seven geomagnetic disturbed periods induced enhancement to SBAS system performance, three reduced the system performance while one does not have effect on SBAS system performance. The present study also confirmed that ROTI is a good proxy to indicate the presence and absence of irregularities in the ionosphere at low latitudes. It is also a better parameter than geomagnetic indices for the assessment of storm-time effects on GNSS-SBAS performance.
Keywords: GNSS, SBAS, Equatorial Ionosphere, ROTI, Geomagnetic indices, Performance

1. Introduction

Ionosphere is a dynamic plasma region in the Earth's upper atmosphere that varies with solar and geomagnetic activities, geographic locations, seasons and time of the day. It has been shown that equatorial and low-latitude ionosphere is the most complex region with higher variability, with morphology quite different from other latitudes [*Kelley et al., 2006*]. [*Schunk and Sojka, 1996*] showed that when magnetic activity changes rapidly, there is occurrence of prompt penetration of magnetospheric electric field from high to low latitudes and the electric fields induced by the dynamo action of the storm-generated neutral winds appear in the equatorial region. [*Blanc and Richmond, 1980*] indicate that when geomagnetic activity increases, the equatorial ionosphere displays high variability in response to the prompt penetration of transient magnetospheric electric fields into low-latitude ionosphere and electric fields generated by the ionospheric disturbance dynamo. Ionospheric electron density irregularities increase due to the injection of the high energetic particles from the sun into the magnetosphere through the solar wind, and between the magnetosphere and the ionosphere results into ionospheric stormness which disrupt radio-waves propagation.

[*Aarons, 1991*] indicate that geomagnetic storm can either increase usual equatorial post-sunset ionospheric electron density irregularities activity or inhibit them depending on the local time of the storm occurrence. [*Manisilla, 2014*] studied some ionospheric storm effects at equatorial and low latitudes regions during intense geomagnetic storms and concluded that ionospheric storm-time effect in the Equatorial Ionospheric Anomaly (EIA) region need further studies in the case of moderate storms to gain a better knowledge of the ionospheric response to these storms.

The storm-time winds are of importance in the EIA region because of its unique characteristics and mechanisms; they modify the fountain effect that characterizes that region, and transports upper atmosphere composition changes toward low latitudes.

Limited work has been done on SBAS system performance during the geomagnetic storms especially in the equatorial and low latitudes region. [*Hernandez-Pajares et al., 2005*] investigated EGNOS Test Bed (ESTB) ionospheric corrections under the severe geomagnetic storms of October and November 2003 over European middle-latitudes. They found that the ESTB performance was degraded significantly during the storms.

This paper analyse GNSS experimental data to investigate the SBAS system performance during the periods of seven minor/weak and moderate geomagnetic storm events of July and October 2013 in the African equatorial and low-latitude region.

2. Data and method of analysis

The data used were obtained from the ground-based GNSS receiver stations within the Northern and Southern crest of the African Equatorial Ionization Anomaly (EIA) region, for the month of July and October 2013. The details of the coordinates of the GNSS stations used are given in Table 1. The stations were divided into two groups based on their local time. Group A has its local time equal to coordinated universal time (LT = UT). It comprises of Ouagadougou, Yamoussoukro, Dakar, and Sao-Tome while Group B local time is one hour ahead coordinated universal time (LT = UT + 1). It comprises of Toro, Yola, Kebbi, Enugu, Cotonou and Libreville.

The variations of Dst (disturbed storm time) index, a measure of geomagnetic activity that determine the severity of the magnetic storm and ring current energy density in equatorial and low-latitude region, was used to analyse the geomagnetic storm as function of local time. Following the terminology of [*Sugiura and Chapman*, *1960*], geomagnetic storms are classified into minor/weak with Dst between -50 nT and -30 nT; moderate storms fall within Dst -50 nT and -100 nT; and great/intense storms are with Dst < -100 nT.

In order to illustrate the geomagnetic storm effect on the ionosphere, the transient variation of rate of change of total electron content index (ROT) and rate of change of TEC index (ROTI) were estimated using Equations 1 and 2 respectively. These parameters measure the level of equatorial ionospheric gradient and irregularities as described by [*Pi et al.*, *1997*]. These parameters were used by [*Jiyun et al.*, *2006*] to estimate the presence of temporal gradients. [*Pi et al.*, *1997*] defined ROTI as a GPS-based index that characterised the severity of the fluctuations, detects the presence of ionospheric irregularities and irregular structure of TEC spatial gradient. [*Basu et al.*, *1999*] referred to ROT as a good proxy to estimate ionospheric scintillation. [*Chandra et al.*, *2009*] as well used ROT and ROTI to identify the signals which suffer severely from ionospheric gradient.

$$ROT = \frac{TEC_k^i - TEC_{k-1}^i}{t_k - t_{k-1}} \tag{1}$$

$$ROTI = \sqrt{< ROT^2 > - < ROT >^2} \tag{2}$$

where i is the visible satellite and k is the time of epoch, TEC is the total electron content, ROT is the rate of change of TEC and ROTI is the change of change of TEC index (five minutes standard deviation of ROT at a sampling interval of 30 s).

An index of ionospheric disturbance DvTEC (Equation 3), the percentage of the relative deviation of the vertical TEC from the quiet reference level for each station was calculated, to look for the positive and negative phases of the storms. The monthly mean of vTEC for the 10 quietest days of each month was used as quiet reference level. The ionosphere is assumed pierced at 350 km height for the calculation of vertical TEC from slant TEC. The increase in DvTEC values (positive phase of the storm) correspond to increase in ionisation associated to the storm effect that limit the occurrence or inhibit the post-sunset irregularities while decrease in DvTEC values (negative phase of the storm) correspond to the depletion of the ionisation associated to the storm effect, this enhances the irregularities at the post sunset to midnight periods.

$$DvTEC = \frac{vTEC_d - vTEC_q}{vTEC_q} \times 100 \tag{3}$$

where DvTEC is the relative percentage deviation of vertical TEC from the reference level, $vTEC_q$ is the reference level (monthly mean of vTEC for the most 10 quietest days of the month of the storm), $vTEC_d$ is the vTEC of the disturbed day.

To illustrate the effects of the geomagnetic storm-time on SBAS system performance, availability maps according to APV-1 level of service (Approach with Vertical Guidance level of service 1) are used. These maps represent the percentage of epochs in a day that the horizontal and vertical Protection Levels (PLs) are below the horizontal and vertical Alarm Limits (ALs) [HPL < 40 m and VPL < 50 m]. These parameters are defined in ICAO SARPs (Standard Aviation Requirement Procedures) as operational rules and procedures for user to use the SBAS system for civil aviation application. SBAS APV-1 availability maps were obtained using specific low-latitude algorithm SBAS emulator (magicSBAS platform) developed by GMV and acquired by ICTP for TREGA project.

Three days were used for each of the storms considered: the day before the storm or the day in which the storm commenced, the main phase of the storm and the day after the storm to study the evolution of the storm and its effect on SBAS system performance.

Table 1: GNSS stations and their coordinates used.

ID	Location	Geo. Lat (^{o}N)	Geo. Lon (^{o}E)	Modip (^{o})
NG2	Toro (Nigeria)	10.12	9.12	-1.96
AF2	Ouagadougou (Burkina Faso)	12.35	-1.51	2.86
NG1	Yola (Nigeria)	9.35	12.50	-3.34
NG4	Kebbi (Nigeria)	12.47	4.23	3.50
AF5	Yamoussoukro (Cote d'Ivorie)	6.87	-5.24	-10.63
NG3	Enugu (Nigeria)	6.42	7.51	-10.89
AF3	Cotonou (Benin)	6.23	2.27	-11.83
AF1	Dakar (Senegal)	14.75	-17.49	11.86
AF6	Libreville (Gabon)	0.35	9.67	-23.90
AF4	Sao-Tome (Soa-Tome)	0.34	6.73	-24.60

3. Results and Discussion

3.1 Geomagnetic Storm of July 5-7 2013

Figs. 1(a-c) show the analysis of the moderate geomagnetic storm of July 6 2013 with the plots of Dst, DvTEC, ROTI and SBAS APV-1 availability maps. The uppermost panel in Fig. 1a and Fig. 1b left indicate the commencement of the storm with Dst -57 nT at 0600 LT (0700 LT) on July 6 and its maximum downward excursion of -79 nT at 1800 LT (1900 LT) in group A (group B) for the same day.

The DvTEC values show mostly positive phase of the storm at post sunset to post-midnight and pre-sunrise periods in all the stations with averaged 100 % vertical TEC enhancement except few stations like Toro where positive phase reached 300 % at 0600 LT (0700 LT) on July 5 (a day before the storm) at pre-sunrise hours, and recovered before 0700 LT (0800 LT), then later increased to 200 % on the same day at post sunset hours. The pre-storm enhancement in both TEC and critical frequency of F2-layer (foF2) was previously observed by [*Danilov, 2001; Araujo-Pradere and Fuller-Rowell 2002; Kane 2005*]; Last author associated this behavior to the meteorological influence. Positive phase of the storm is also observed on the day of the storm at post mid-night and post sunset in Fig. 1b except stations like Toro, Yola and Cotonou that show some fluctuations to negative phase which could be due to receiver's noise that could not be filtered out. The positive phase effect could be assumed to the prompt penetration of the magnetospheric electric field to the ionospheric height during the magnetic disturbance as suggested by [*Wolf et al., 2007*; *Sun et al., 2012*]. However, there is some decrease in vertical TEC on the day before and the day after the storm at some stations near or on the southern crest of anomaly. These are pre-storm and post-storm effect associated to the reduction in O/N_2 ratio in the thermospheric gas as explained by [*Sun et al., 2012*].

Low values of ROTI at post sunset to midnight is an indication of ionospheric irregularities inhibition while high values of ROTI at post sunset period indicates presence of ionospheric irregularities, a normal phenomenon at equatorial and low latitude regions. It is clear from Fig. 1b that ionospheric irregularities are inhibited in all the stations considered. The inhibition of ionospheric irregularities during the increase geomagnetic activity was explained by [*Aarons, 1991*], he associated them to a local time effect. If the height of the F-layer is disturbed during the daytime LT (0700-1800), ionospheric irregularities are inhibited; on the contrary if disturbances are at midnight to pre sunrise (1200-0600) LT, irregularities are generated and enhanced. Thus, in the days before and after the storm, irregularities are observed in Yamoussoukro, Enugu, Cotonou, Libreville and Sao-Tome at the post sunset hours. These stations are located near or on the southern crest of anomaly, indicating that the pre-storm and post-storm effects are more pronounced in southern hemisphere than the northern hemisphere. The disturbance through the injection of magnetospheric electric field into ionospheric height during the geomagnetic activity of July 6 could have altered the global thermospheric circulation, and consequently altered the generation of electric fields and current at middle and low latitudes by ionospheric wind dynamo action.

The signature of the irregularities inhibition is clearly seen in the performance of SBAS APV-1 availability maps presented in Fig. 1c The SBAS APV-1 availability reached 99 % on July 6 in a larger area, indicating enhancement in the SBAS system performance (Fig. 1c middle). However, the coverage area is reduced on July 5, the day before the storm and July 7, the day after the storm to 95% and 90% availability respectively around the stations where the ionospheric irregularities are not inhibited at the post sunset period to mid-night hours as seen in Figs. 1c left and right respectively.

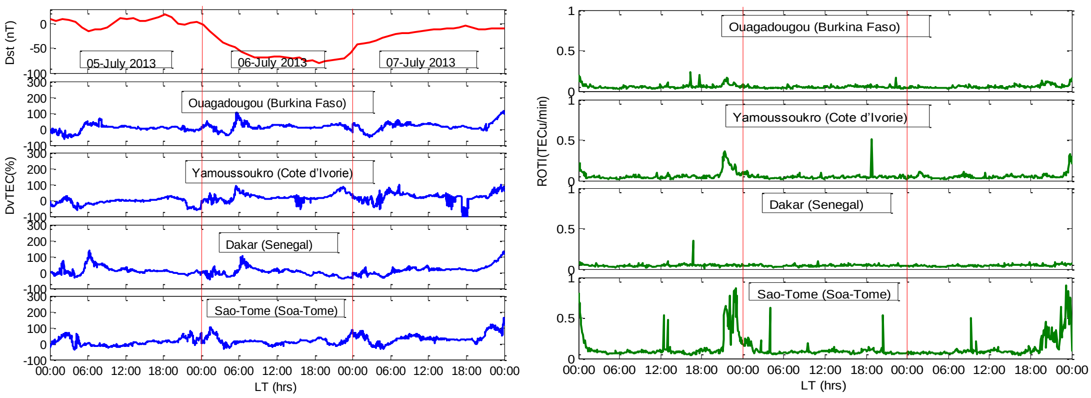

Fig.1a: Variations of Dst (red), DvTEC (blue) and ROTI (green) for group A

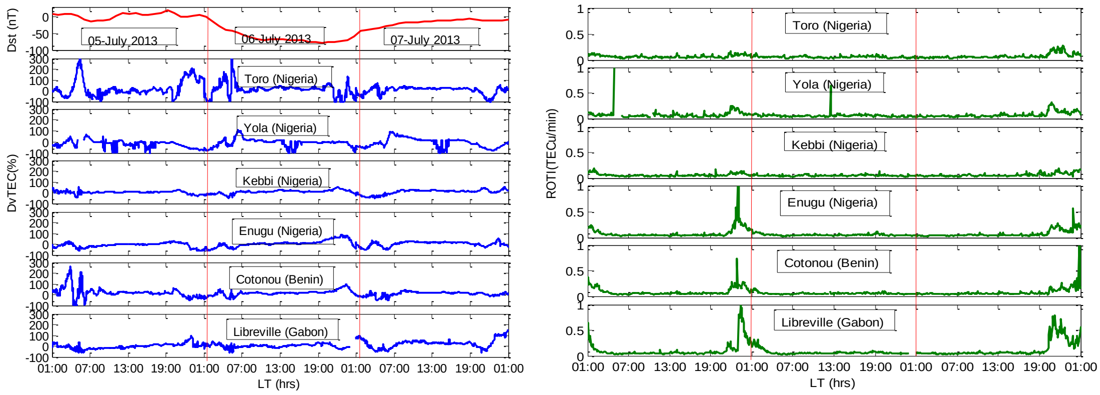

Fig.1b: Variations of Dst (red), DvTEC (blue) and ROTI (green) for group B

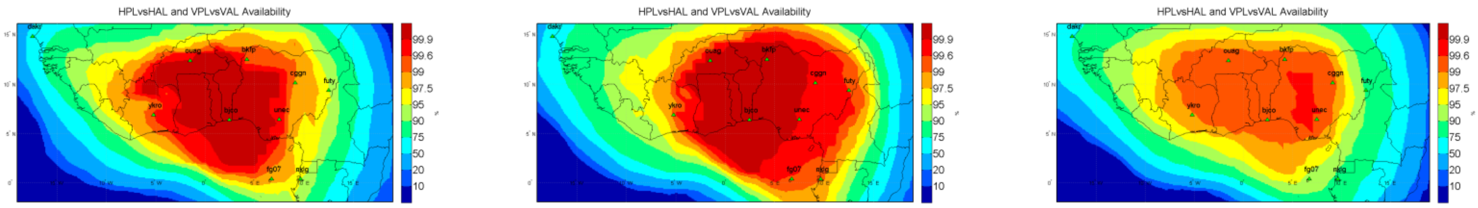

Fig 1c: SBAS APV-1 availability maps for July 5 (left), July 6 (middle) and July 7 (right) 2013

3.2 Geomagnetic Storm of July 9-11 2013

Figs. 2 (a-c) show the situation that corresponds to July 9-10 minor/weak geomagnetic storm and its impact on SBAS system performance. The storm commenced its downward excursion on July 10 with Dst -31 nT at about 0500 LT (0600 LT) and reached minimum of -47 nT about 2100 LT (2200 LT) the same day in group A (group B) as indicated in Figs. 2a and 2b, after which it began upward recovery to the following day. It is clearly seen that the daytime (sunrise to sunset) vertical TEC is not so much deviated from the quiet period. Little increase and decrease (positive and negative storm effect) in vertical TEC at the pre-sunrise to pre-midnight of the day before the storm commenced and the 10th of July, the main phase of the storm, on the stations (Yamoussoukro, Enugu, Cotonou, Libreville and Sao-Tome) near or on the southern crest of anomaly regions.

Furthermore, in order to see the influence of the storm on the development and inhibition of equatorial ionospheric irregularities activity, the transient variations of ROTI plots are presented in Figs. 2 (a and b) right for all the stations used. A smooth variation of ROTI is observed in Dakar, a location towards the Northern crest of equatorial anomaly before and during the storm of July 10. On the same days, the magnitude of ROTI during the post sunset periods of the stations located near/on the trough of anomaly (Ouagadougou, Toro, Yola and Kebbi) is quite similar and small. But high values of ROTI are observed on day before and during the storm at the post sunset hours at the stations near/on the Southern crest of equatorial ionisation anomaly (Yamoussoukro, Enugu, Cotonou, Libreville and Sao-Tome). From the Figs. 2 (a and b) right, it is observed that ionospheric irregularities decreased toward the Northern crest and increased towards the Southern crest of the equatorial anomaly on the day before and during the storm. The recovery day of the storm have nearly similar behaviour in all the station, the ROTI values at post sunset hours are very low. The inhibition observed at the station in Dakar before and during the magnetospheric disturbed periods could be associated to the longitudinal effect induced by meridional and zonal neutral winds.

The effect of the behavior of the ionospheric irregularities is seen in the SBAS APV-1 availability maps presented in Figs. 2c. Fig. 2c left shows the SBAS APV-1 availability map for July 9, a day preceded the storm; the 99 % coverage area is reduced at the stations located near/on the Southern crest of equatorial anomaly to 95 %. On the day of the storm, the SBAS system performance went down to 75 % as seen in SBAS APV-1 availability map (Fig. 2c middle), this indicates that SBAS system is more degraded during the geomagnetic storm of July 10. However, an enhancement in SBAS system performance to 99 % availability is observed on July 11 (Fig. 2c right), a recovery day of the geomagnetic storm when the irregularities is lowered/disappeared during the local post sunset to midnight periods except the few stations at the edge of service area.

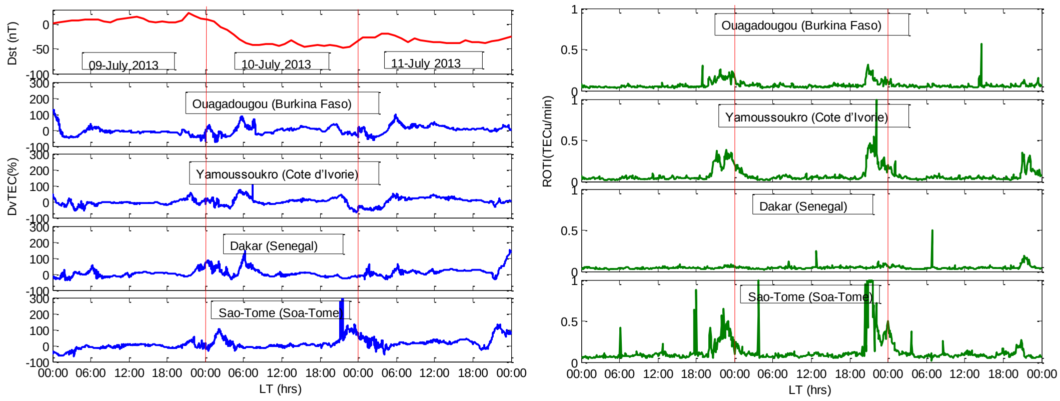

Fig.2a: Transient variations of Dst (red), DvTEC (blue) and ROTI (green) for group A

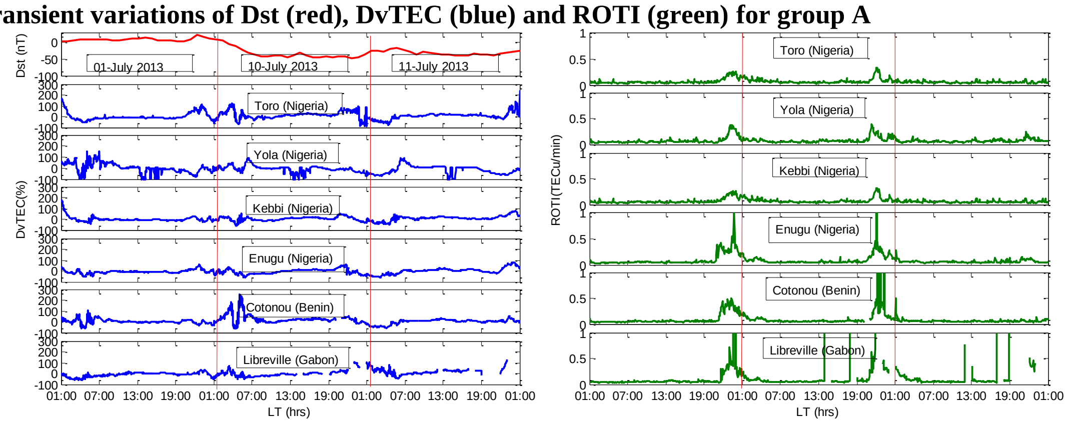

Fig.2b: Transient variations of Dst (red), DvTEC (blue) and ROTI (green) for group A

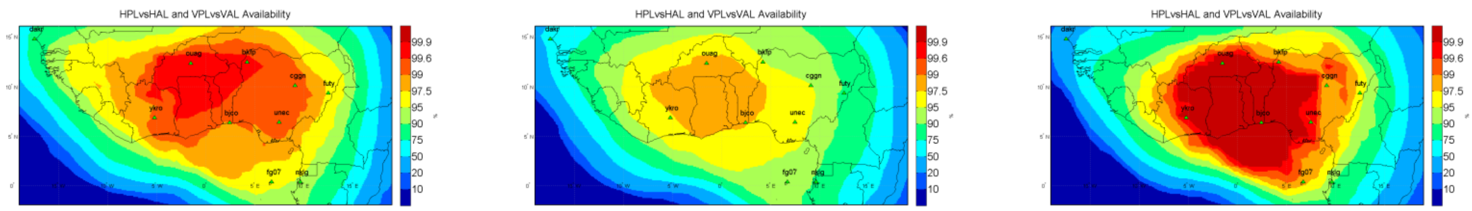

Fig 2c: SBAS APV-1 availability maps for July 9 (left), July 10 (middle) and July 11 (right) 2013

3.3 Geomagnetic Storm of July 13-15 2013

Figs. 3(a-c) present the analyses of the moderate storm of July 13-15 and it effect on SBAS system performance. The storm initialised its evolution on July 14 at 1300 LT (1400 LT) with Dst -38 nT and reached its maximum downward excursion at about 2200 LT (2300 LT) the same day with Dst -72 nT, then started recovery phase at about midnight 1200 LT (0100 LT) to the following day but maintained ~ -40 nT till the post sunset of the same day (15th July) as presented in upper panel of Fig. 3a and Fig. 3b left. The DvTEC values in Figs. 3(a and b) almost followed the same pattern of variations in the three days in all the stations with increase and decrease in TEC values at post sunset to midnight and post mid-night to pre-sunrise but stable during the daytime (0600-1900 LT). Pre-storm increase inTEC is not so common here unlike July 6 moderate storm. Similar trend ~100 % (~200 %) vertical TEC enhancement is observed at Ouagadougou (Yola) on the day before, during and after the storm between 0500LT and 0700 LT, no increase nor decrease of TEC at post sunset to midnight hours as seen in Fig. 3a second panel. Fig. 3a fifth panel shows the DvTEC at Sao-Tome, ~ 50 % vertical TEC increment (positive phase of the storm) is observed at post mid-night and post sunset periods, on the following day (July 15, the recovery day) ~ -50 % vertical TEC decrease (negative phase of the storm) at about 0300 LT and suddenly rose to 100 % TEC (positive phase) at 0500 LT and 200 % TEC (positive phase) during post sunset to midnight. Fig. 3b seventh panel presents the DvTEC at Libreville, no deviation of TEC from its quiet period for July 13, but TEC fluctuation is observed at the pre-sunrise (0500-0600) LT ~ ±100 % TEC. On the same station, ~ 100% TEC enhancement (positive phase) is observed at 0400 LT and suddenly changed to -100% TEC (negative phase) at 0500 LT on July 15. The TEC measured at Sao-Tome and Libreville stations are prone to fluctuation in TEC at post sunset to post mid-night periods due the physical mechanism of fountain effect producing the crest of anomaly, this has been extensively studied for many decades.

Figs. 3(a and b) right present transient variations of ROTI for the moderate geomagnetic storm understudy. From the Fig. 3a (right), ROTI value is quite low on the day precede the storm's commencement (~0.3 TECu/min), on the day of the storm as well the recovery day (July 15) in Ouagadougou, Yamoussoukro and Dakar except Sao-Tome where there is sudden increase in ROTI (1 TECu/min) at post sunset periods. In the same vein, Fig. 3b (right) presents ROTI of Toro, Yola, Enugu, Cotonou and Libreville. The magnitude of ROTI is low in all the days for all the stations except Libreville. The fluctuations of TEC at the Southern crest of anomaly are clearly shown in the ROTI plots. The highest values are recorded in Sao-Tome and Libreville during the post sunset hours (~0.8-1.0) TECu/min on the day before, during and after the increased geomagnetic activity. In general, there are more irregularities on the July 14, the main phase of the storm and July 15, the recovery phase. This is contrary to Aarons' third criterion about non effect of the storm on the post sunset ionospheric irregularities when the Dst maximum excursion occurs after local sunset (Aarons, 1991).
The effect of the geomagnetic storm is seen in the SBAS APV-1 availability map shown in Fig. 3c. It is clearly seen in Fig. 3c (left) that SBAS system performance is not affected by the geomagnetic storm of July 13, but the system is degraded to 75 % availability on the July 14 and 15, during and after the geomagnetic storm (Fig. 3c) middle and right panel respectively.

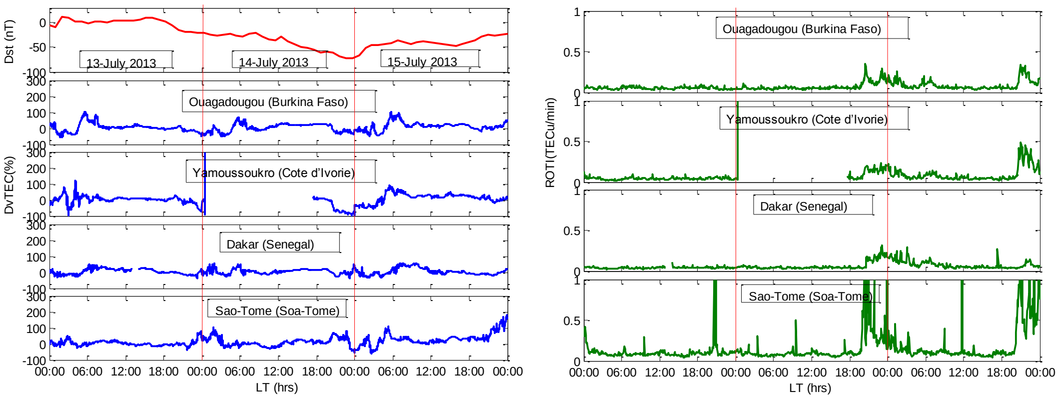

Fig.3a: Transient variations of Dst (red), DvTEC (blue) and ROTI (green) for group A

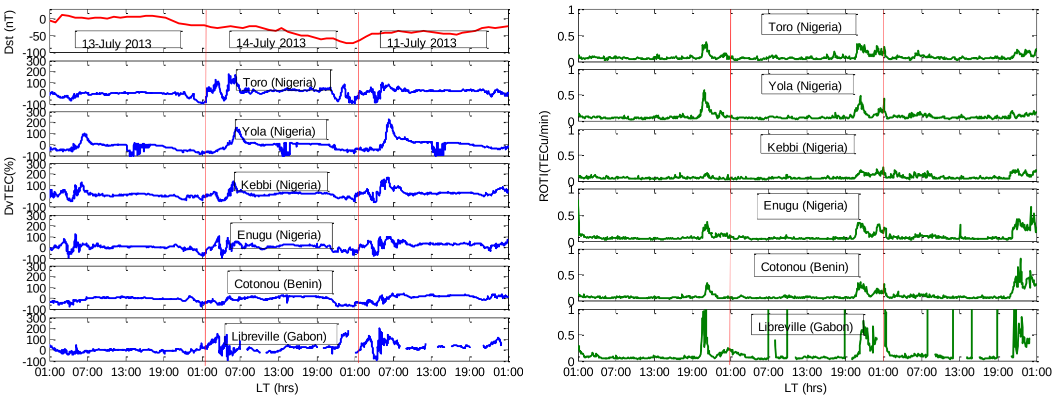

Fig.3b: Transient variations of Dst (red), DvTEC (blue) and ROTI (green) for group B

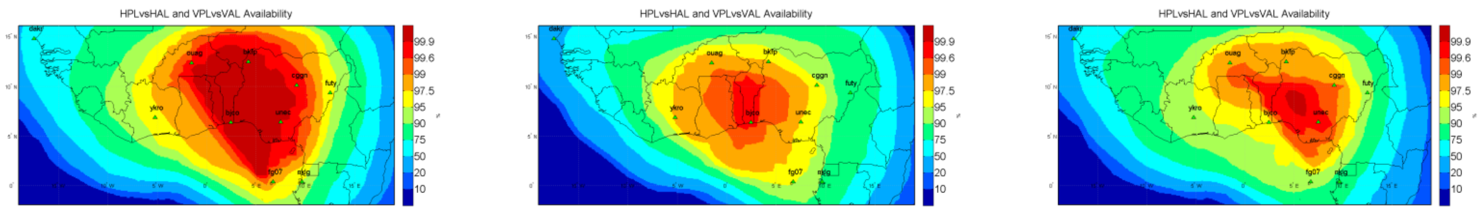

Fig 3c: SBAS APV-1 availability maps for July 13 (left), July 14 (middle) and July 15 (right) 2013

3.4 Geomagnetic Storm of October 1-3 2013

Figs. 4(a-c) show the situation that corresponds to a moderate geomagnetic storm and the corresponding SBAS system performance analyses. The storm commenced suddenly at 0300 LT (0400 LT) for group A (group B) on October 2 (Figs. 4(a and b) left). It had its Dst maximum downward excursions of -67 nT at 0700 LT (0800 LT) for group A (group B).

The storm seems not to have effect on the vTEC on October 1, a day preceded the storm. However, the ionosphere (vertical TEC) over group A stations responded immediately to the shock impacted by the storm, steep down to ~ -80 TEC unit (negative phase of the storm). The ionospheric system then recovered with uniform steep increased to ~100 % TEC unit (positive phase of the storm) at the maximum downward excursion -67 nT. All the stations in group A are observed to have enhancement in vTEC at the post sunset hours except Ouagadougou where there is ~ -50 % TEC depletion at 2100 LT but picked up before midnight with ~ 200 % TEC to midnight. The vertical TEC of all the stations in Group B fluctuates in a similar way except the stations at Yola and Enugu, which appear be too noisy. In general, DvTEC plots show that positive and negative phases of the storm are mostly at the post sunset to pre sunrise periods during and after the storm.

Figs. 4(a and b) right, present ROTI over all the stations used. The day before, during and after the increased geomagnetic activity have the same range of behaviours of ~ 0.9 TECu/min at the post sunset to midnight periods in all the stations except Dakar that has lower value of ROTI ~ 0.5 TECu/min on October 2, the day of the storm. There is no increase in normal ionospheric irregularities activity as shown by ROTI before, during and after the moderate storm indicating that the storm has neither enhancement nor inhibition on the irregularities activity.

The SBAS APV-1 availability maps presented in Fig. 4c shows SBAS system performance before, during and after the storm event. The SBAS system performance for these days is of the same range from 75 % to 95 % availability, indicating that the geomagnetic storm of October 1-3 has no effect on system performance due to the non-effect of the storm on irregularities activity during those periods.

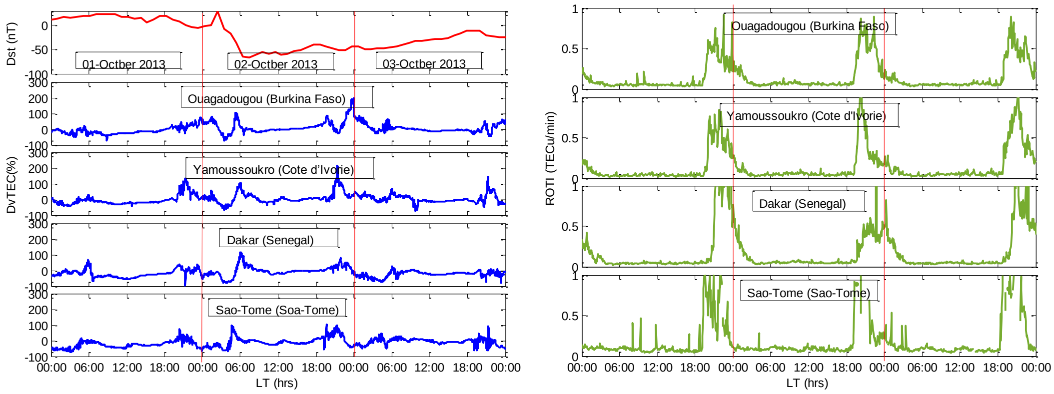

Fig.4a: Transient variations of Dst (red), DvTEC (blue) and ROTI (green) for group A

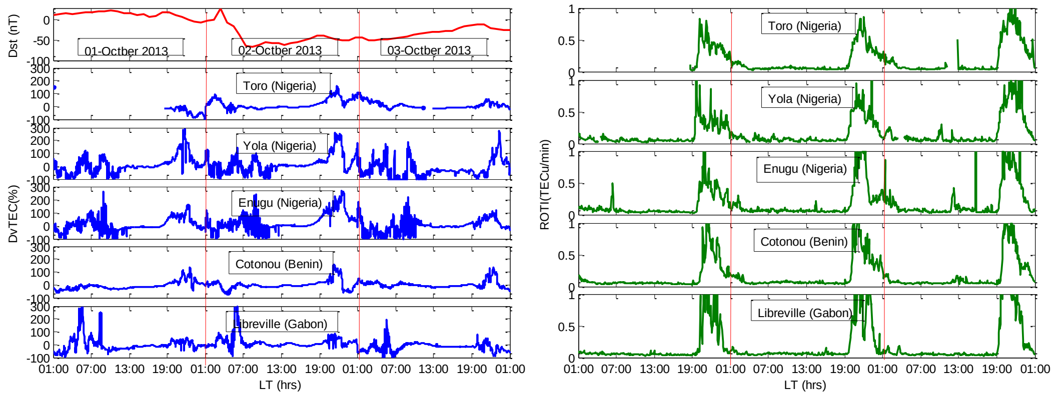

Fig.4b: Transient variations of Dst (red), DvTEC (blue) and ROTI (green) for group B

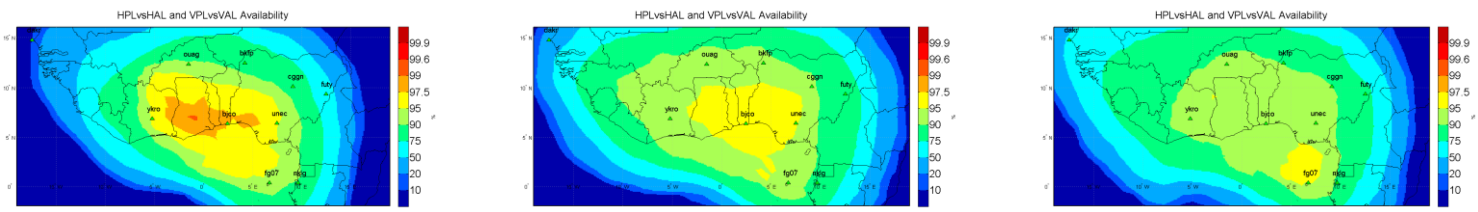

Fig 4c: SBAS APV-1 availability maps for October 1 (left), October 2 (middle) and October 3 (right) 2013

3.5 Geomagnetic Storm of October 8-10 2013

Figs. 5(a-c) present the analyses of the moderate geomagnetic storm of October 8-10 and its impact on SBAS system performance. It is shown from Figs. 5(a and b) left uppermost panel that the storm commenced on October 8 at 2200 LT (2300 LT) with Dst -30nT and reached its Dst maximum downward excursion -65 nT at 0100 LT (0200 LT) for group A (group B) on October 9 2013. The storm began it recovery at 0800 LT (0900 LT) for group A (group B) on the same day though maintain low values of Dst till the following day.
The DvTEC fluctuates more on the onset of the storm in response to the ring current decrease, DvTEC exhibits both increase and decrease (positive and negative phases) in all the stations observed. There is much increase in TEC (~ 100 % positive phase) at pre sunrise hours on October 10 during the recovery phase of the storm in all the stations. This is followed by a drastic sharp decrease in TEC (-50 % negative phase) at 0500 LT (0600 LT) on October 10 when the Dst went down again from -28 nT to -38 nT. It is as well observed that vTEC fluctuates more at the post sunset to pre sunrise periods and relatively stable during the daytime.
The rate of change of TEC index (ROTI), during the period October 8-10 is given in Figs. 5(a and b) right. The midnight to post mid-night period of the October 8 has low value of ROTI indicating that there is no ionospheric irregularities at midnight. However, there occurred irregularities after sunset to post midnight and even pre sunrise (0500 LT) in some locations. Also the magnitude of ROTI on October 9 post sunset period is high. This is in agreement with Aarons' second criterion about the increase in ionospheric irregularities activity when the maximum Dst downward excursion occurs after local midnight to post mid-night (Aarons, 1991). Though the level of irregularities are not the same, more in group A stations and less at post sunset period of the station on the equatorial anomaly trough.
The signature of the increased irregularities is observed in the Figs 5c showing SBAS APV-1 availability maps. The SBAS system performance on October 9 when there is increased in ionospheric irregularities at the pre sunrise and post sunset due to geomagnetic storm is degraded to 50 % availability (Fig. 5c middle) and the SBAS system coverage area is small in comparison to October 8 and 10 (see Figs. 5c left and right respectively).

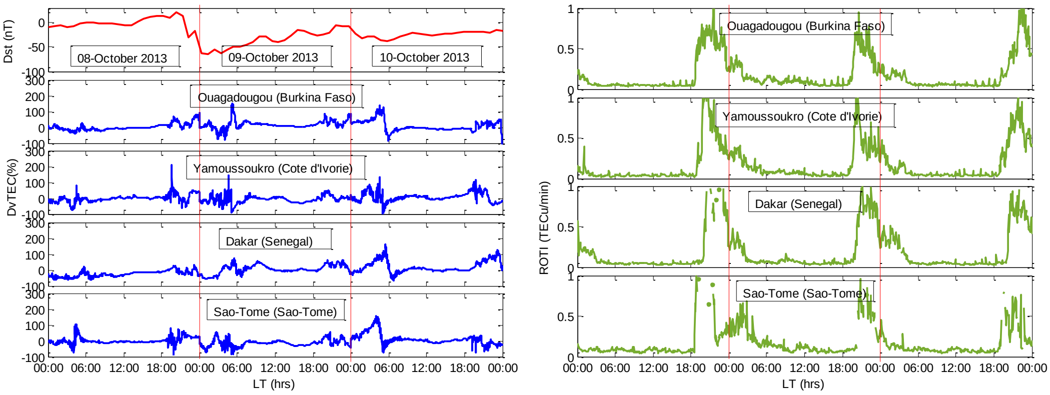

Fig.5a: Transient variations of Dst (red), DvTEC (blue) and ROTI (green) for group A

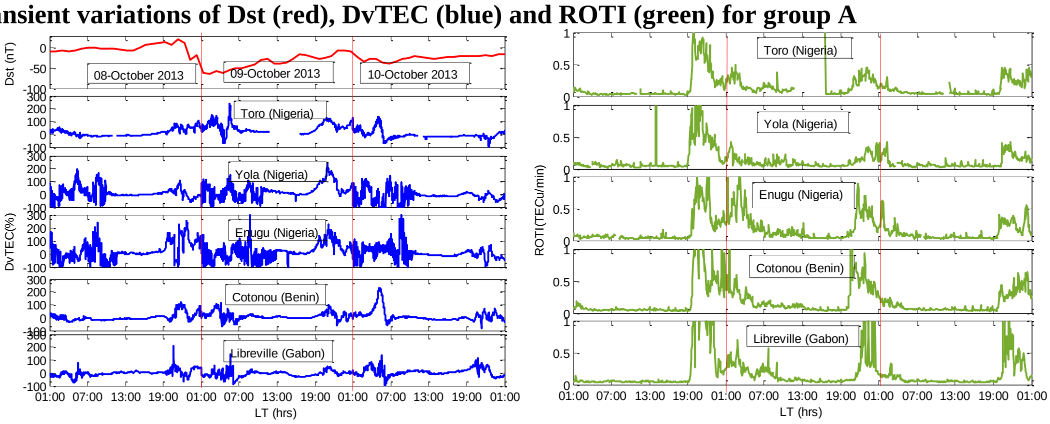

Fig.5b: Transient variations of Dst (red), DvTEC (blue) and ROTI (green) for group B

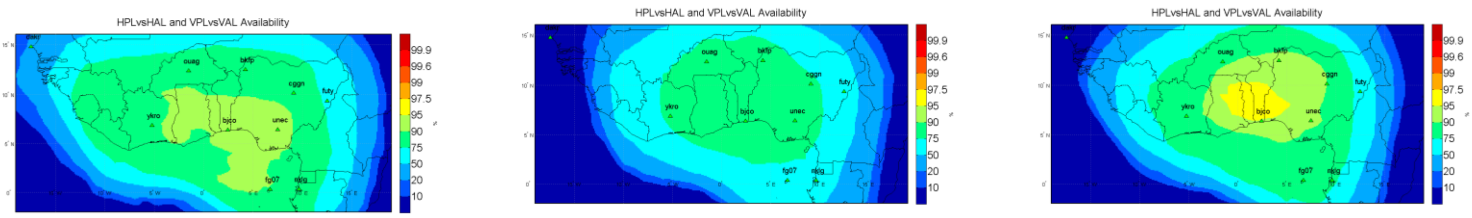

Fig 5c: SBAS APV-1 availability maps for October 8 (left), October 9 (middle) and October 10 (right) 2013

3.6 Geomagnetic Storm of October 13-15 2013

Figs. 6(a-c) show the situation that corresponds to the minor/weak geomagnetic storm and its impact on SBAS system performance that occurred on the above mentioned periods. The magnetosphere was disturbed as shown in Figs. 6(a and b) when the Dst jumped from 8 nT to -3 nT on October 14 at 1000 LT (1100 LT) and reached maximum downward excursion at 0300 LT (0400 LT) in group A (group B) on October 15 the following day. There is increment in relative TEC ~100 % (positive phase) in all the stations in group A at 0500 LT (pre sunrise) on 13 October, except Yamoussoukro which has its own equivalent magnitude of TEC enhancement at 2100 LT (post sunset). On the same day, ~70 % TEC increased is observed at Sao-Tome at 2100 LT. On October 14, the relative TEC increased ~ 300 in all the stations at post sunset hours except the stations on the crest of anomaly having ~ 100% increased at the post sunset to midnight.

The influence of the night-time increase in TEC of the October 14 is seen in ROTI plots of Figs. 6 (a and b) right. The ROTI value is uniformly low ~ 0.075 TECu/min in all the stations at post sunset to midnight, indicating that the usual post sunset to post midnight irregularities are inhibited. This is similar to Aarons' criterion one saying when the Dst excursion maximises during the daytime, irregularities activity is inhibited.

The effect of the storm-induced inhibition and increased irregularities are presented in SBAS APV-1 availability maps shown in Fig. 6c. The day preceded to the storm has usual post sunset irregularities; the SBAS system performance reached 95 % availability (Fig. 6c left). While on the 14 of October, the irregularities are inhibited and the SBAS system performance reached 99 % availability (see Fig 6c. middle). But the SBAS performance reduces to 90 % availability due to the presence of irregularities at the post sunset to midnight of October 15 (Fig. 6c right).

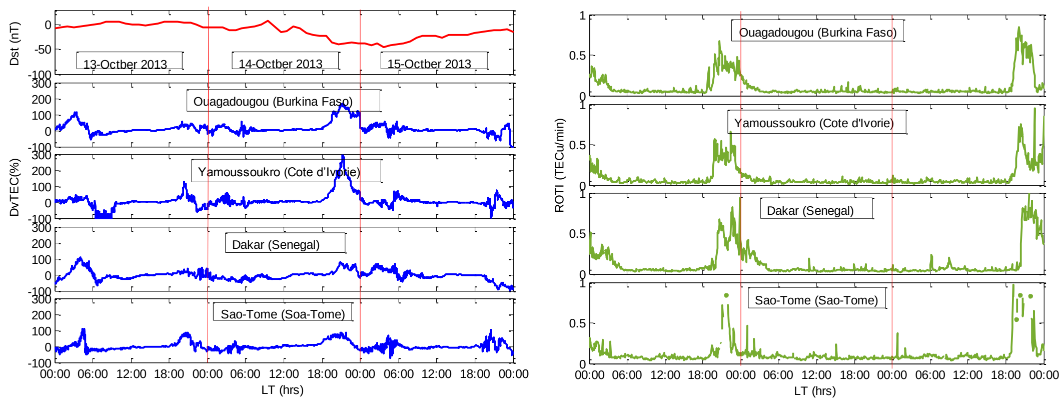

Fig.6a: Transient variations of Dst (red), DvTEC (blue) and ROTI (green) for group A

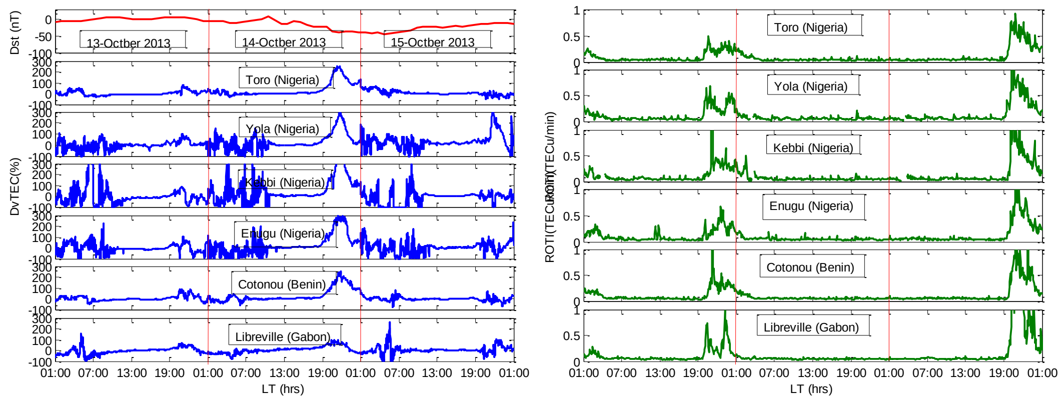

Fig.6b: Transient variations of Dst (red), DvTEC (blue) and ROTI (green) for group B

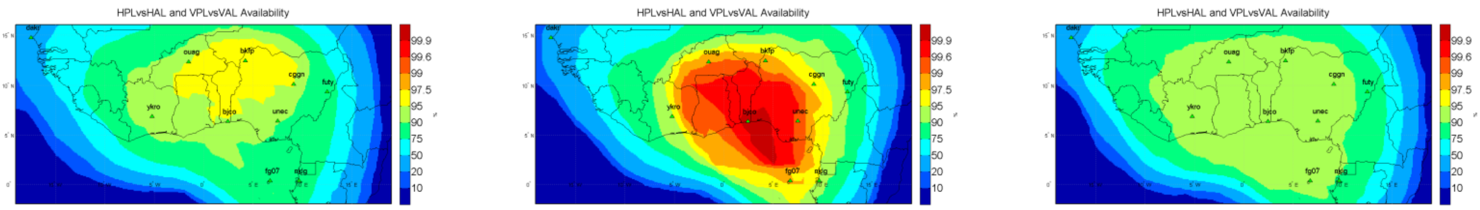

Fig 6c: SBAS APV-1 availability map for October 13 (left), October 14 (middle) and October 15 (right) 2013

3.7 Geomagnetic Storm of October 29-30 2013

Figs. 7 (a-c) present the situation that corresponds to October 29-31 moderate geomagnetic storm and its impact on SBAS system performance. From Fig. 7a and Fig. 7b left, it is observed that the storm commenced on October 30 at 0700 LT (0800 LT) when the Dst jumped from 4 nT to –5 nT and reached its maximum downward excursion -52 nT at 2300 LT (0000 LT) for group A (group B) on October 30 2013 (October 31). Then began its upward recovery at 1100 LT (1200 LT) for group A (group B) on October 31. In the same Figs., the TEC deviation fluctuates as usual in post sunset to post midnight and stable during the sunrise to sunset hours (daytime) but a sporadic fluctuation is observed on October 30 in a station Sao-Tome.

In Figs. 7(a and b) right, the irregularities observed on the day preceded the storm after sunset is higher in group A stations with an average ~0.9 TECu/min than group B average ~0.5 TECu/min. Except Libreville station with 1TECu/min, being a station on the crest of equatorial anomaly region. The pre-storm effect differences could be due to differences in local and geographic longitude. On October 30, the ionospheric irregularities are reduced (inhibited) in all the stations at the crest (trough) of equatorial anomaly.

The storm effect on the ionosphere is observed in the SBAS system performance presented in SBAS APV-1 availability maps (Fig. 7c). The SBAS system performance on October 29 could not exceed 90 % availability due to the influence of irregularities at post sunset to post midnight periods. The performance increased to 99.6 % availability on October 30 when the irregularities are lowered (inhibited) at the crest (trough) of equatorial anomaly. Then the performance further degraded to 90 % on October 31 as the irregularities resurface during post sunset to midnight.

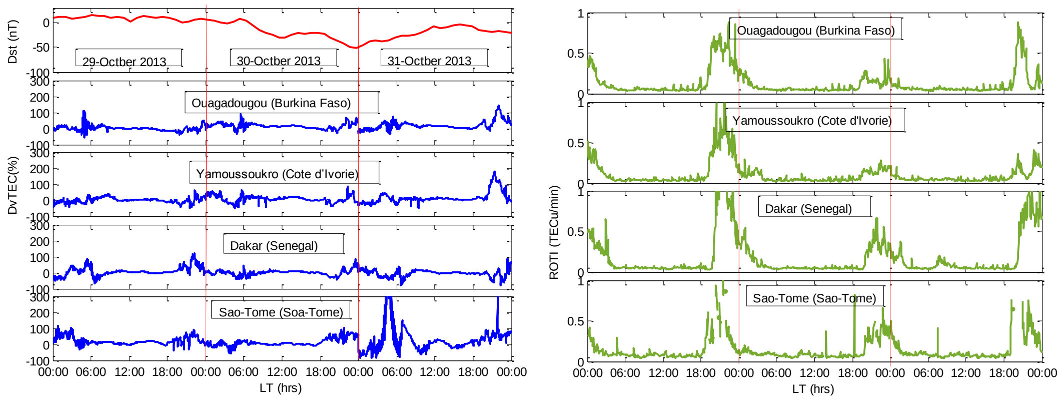

Fig.7a: Transient variations of Dst (red), DvTEC (blue) and ROTI (green) for group A

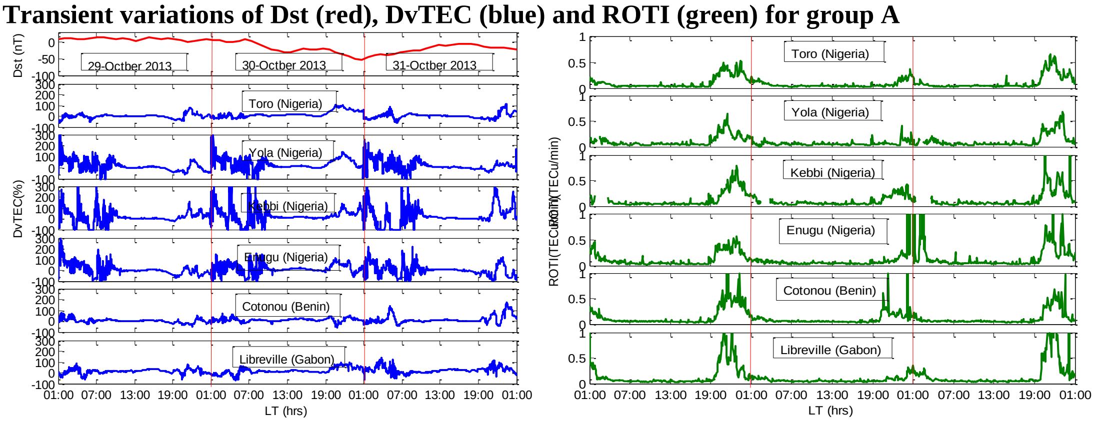

Fig.7b: Transient variations of Dst (red), DvTEC (blue) and ROTI (green) for group B

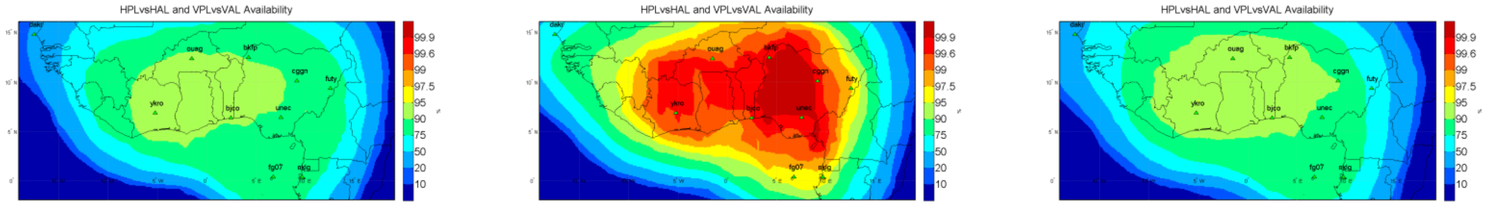

Fig.7c: SBAS APV-1 availability map for October 29 (left), October 30 (middle) and October 31 (right) 2013

4.0 Conclusions

This study assessed the effect of the ionosphere at African low-latitudes on SBAS system performance using real GNSS data stations from African equatorial latitudes and a EGNOS-like algorithm during seven disturbed geomagnetic conditions: two minor/weak with Dst ≥ -50 nT and five moderate with -50 nT ≤ Dst ≥ -100 nT. Both positive (increase in vTEC) and negative (decrease in vTEC) phases of the disturbed conditions effects are observed at African equatorial and low-latitude region, mostly during post sunset and pre sunrise periods. Though positive phases are more frequent than negative; positive phases are considered to be induced by the disturbance dynamo field penetration within the ionospheric current system and the penetration of the magnetospheric electric field and current to the ionosphere, while negative phases are assumed to be due to the decrease in O/N_2 ratio in the upper atmosphere. These effects modify the morphology and the physics of the ionosphere at post sunset to post mid-night periods leading to inhibition or increase of ionospheric irregularities. [*Aarons, 1991*] associated the effect to the local time in which the storm occurs (“Aaron’s criterion”). This research shows that this criterion appears to be true in some of the disturbed periods analysed while other case do not correspond to it. The SBAS system behaviour during an increased geomagnetic activity is quite complex and cannot be based only to geomagnetic indices and depends on specific conditions that influence the occurrence of ionospheric irregularities. The present study reveals that ROTI is a good proxy to indicate such occurrence also during geomagnetic disturbed conditions showing clearly increase or inhibition of irregularities. ROTI is a good indicator of SBAS performance: it indicates enhancements in the system performance when inhibition of usual ionospheric irregularities activity is observed and degradations in system performance when increase of irregularities activity is observed. During the storm-time conditions considered, three out of seven geomagnetic storm induced enhancement to SBAS system performance, three reduced the system performance while one does not have effect on SBAS system performance.

Acknowledgements
This paper contains results obtained during the “training through research" activities of the TREGA Project financed by the European Union under the Contribution Agreement between The European Commission and the ICTP.

References

Pi, X., Mannucci, A. J., Lindqdwister, U. J., Ho, C. M. (1997): Monitoring of Global Ionospheric Irregularities using the worldwide GPS. Geophys. Res. Letters, 24, (18), 2283-2286. *Dio/10.1029/97GL02273*

Chandra, K. R., Strinivas V. S., Sarma, A. D. (2009): Investigation of Ionospheric Gradients for GAGAN application. Earth Planets Space, 61, 633-635. *www.**terr**apub.co.**jp/journals**/EPS/pdf/2009/6105/61050633.pdf*

Basu, S., Grove, K. M., Quinn, J. M., Doherty, P. (1999): A Comparison of TEC Fluctuation and Scientillation at Ascension Island. Jour. of Atmos. Solar-Terr. Physics, 61, 1219-1226. *www.sciencedirect.com/science/article/pii/S1364682699000528*

Jiyun, L., Pullen, S., Datta-Baruna, Enge, P., (2006): Assessment of Nominal Ionosphere Spatial Decorrelation for LAAS. IEEE/ION PLANS, 506-514. *Koasas.kaist.ac.kr/bitstream/10203/19779/1/059.pdf*

Aarons, J. (1991): The role of the Ring Current in the Generation or Inhibition of Equatorial F Layer Irregularities during Magnetic storm. Radio Science, 26, (4), 1131-1149

Blanc, M. and Richmond, A. D. (1980): The Ionospheric Disturbance Dynamo. Jour. of Geophys. Res. 85, 1669-1686.

Danilove, A. D. and Lastovicka, J. (2001): Effects of Geomagnetic Storms on the Ionosphere and Atmosphere. Int. Jour. of Geomag & Aeron. 2, 209-224.

Kelley, M. C., Makela, J. J., De la Beaujardiere, O. (2006): Convective Ionospheric Storms: A Major Space Weather Problem. Space weather, 4, doi:http://doi/10.1029/2005SW000144.

Schunk, R. W. and Sojka, J. J. (1996): Ionosphere-Themosphere Space weather Issues. Jour. Atmos. Solar-Terr. Phy. 58 (58), 1527-1574.

Manisilla, G. A. (2014): Some Ionospheric Storm Effects at Equatorial and Low Latitudes. Adv. Space Res. 53, 1329-1336.

Wolf, R. A., Spiro, R. W., Sazykin, S., Toffoleto, F. R. (2007): How the Earth's Inner Magnetosphere works: an Evolution Picture. Jour. Atmos. Solar-Terr. Phys. 69,288-302.

Araujo-Pradere, E. A. and Fuller_Rowell, T. J. (2002): Storm: An Emperical storm-time ionospheric correction model, 2 Validation, Radio Science, 37 (5) 1071.

Kane, R. P. (2005): Ionospheric foF2 Anomalies during some intense Geomagnetic Storms. Ann. Geophys. 23, 2487-2499.

Sun, S. J., Ban, P. P., Chen, C., Xu, Z. W. and Zhao, Z. W. (2012): On the Vertical Drift of ionosphere F layer during Disturbance time: Result from ionosonde. Jour. Geophys. Res. 117 A01303

Ionospheric Studies Task Force (ISTF/1) (2012): Ionospheric Effect on GNSS Aviation Operation Issues – First Meeting of Ionospheric Studies Task Force (ISTF/1), (*available as NSP Flimsy14, WGW meeting in Tokyo, Japan 27-29 Feb 2012*), 4-21.

Sugiura, M. and Chapman, S. (1960): the Mophology of Geomagnetic Storms with Sudden Commencement. Abandl. Akad. Wiss., Gotting Math. Phys. K1 (4).

Hernandez-Pajares, M., Juan Zornoza, J. M., Sanz Subbirana, J., Farnworth R. and Soley S. (2005): EGNOS Test Bed Ionospheric Corrections under the October and November 203 Storms. IEEE Trans. on Geosci. and Rem. Sens. 43 (10).